GRID CONNECTED PV BASED BUCK & BOOST CONVERTER FOR MISMATCHED ENVIRONMENTAL CONDITIONS USING PSO MPPT

[1]Kaya Srinivasa Rao (M.Tech) [2] Kiran Kumar Konda (Assistant Professor)

[1,2]MVR College Of Engineering And Technology, Paritala, Krishna, Andhra Pradesh , INDIA

[1]kaya.srinivas@Gmail.Com [2]kkirankumar218@Gmail.Com

ABSTRACT-In this paper, a molecule swarm improvement (PSO)- based MPPT calculation for PV arrays in confounded ecological conditions is proposed. A solitary phase grid associated transformer less photograph voltaic (PV) inverter which can work either in buck or in boost mode, and can separate maximum power at the same time from two sequentially associated subarrays while each of the sub array is confronting diverse natural conditions, is displayed in this paper. As the inverter can work in buck just as in boost mode relying upon the prerequisite, the limitation on the base number of sequentially associated solar PV modules that is required to frame a sub array is enormously diminished. Accordingly power yield from each of the sub array increments when they are presented to various natural conditions. The topological configuration of the inverter and its control procedure are structured so the high frequency components are absent in the regular mode voltage consequently confining the greatness of the leakage current related with the PV arrays inside as far as possible. Further, high working productivity is accomplished all through its working reach. A point by point examination of the system prompting the advancement of its mathematical model is completed. The suitability of the plan is affirmed by performing point by point simulation examines.

Index Terms—Grid connection, Single phase, Transformerless, Buck & Boost based PV inverter, Maximum power point, PSO, Mismatched environmental condition, Series connected module.

I.INTRODUCTION

The major concern of a photo voltaic (PV) system is to ensure optimum performance of individual PV modules in a PV array while the modules are exposed to different environmental conditions arising due to difference in insolation level and/or difference in operating temperature. The presence of mismatch in operating condition of modules significantly reduces the power output from the PV array [1]. The problem with the mismatched environmental conditions (MEC) becomes significant if the number of modules connected in series in a PV array is large. In order to achieve desired magnitude for the input dc link voltage of the inverter of a grid connected transformerless PV system, the requirement of series connected modules becomes high. Therefore, the power output from a grid connected transformerless (GCT) PV system such as single phase GCT (SPGCT) inverter based systems derived from H-bridge [2], [3] and neutral point clamp (NPC) inverter based systems [4], [5] get affected significantly during MEC.

In order to address the problem arising out of MEC in a PV system, various solutions are reported in the literature. An exhaustive investigation of such techniques has been presented in [6]. Power extraction during MEC can be increased by choosing proper interconnection between PV modules [6], [7] or by tracking global maximum power point (MPP) of PV array by employing complex MPP tracking (MPPT) algorithm [6], [8]. However, these techniques are not effective for low power SPGCT PV system. Similarly, reconfiguration of the PV modules in a PV array by changing the electrical connection of PV modules [9], [10] is not effective for SPGCT PV system due to the considerable increment in component count and escalation in operating complexity. In order to extract maximum power from each PV module during MEC, attempts have been made to control each PV module in a PV array either by having a power electronic equalizer [11] or by interfacing a dc to dc converter [1], [12]-[14]. Schemes utilizing power electronic equalizer

require large component count thereby increasing the cost and operation complexity of the system. The scheme presented in [1] uses generation control circuit (GCC) to operate each PV module at their respective MPP wherein the difference in power between each module is only processed through the GCC.

Scheme presented in [12] uses shunt current compensation of each module as well as series voltage compensation of each PV string in a PV array to enhance power yield during MEC. The schemes based on module integrated converter [13], [14] use dedicated dc to dc converter integrated with each PV module. However, the efficiency of the aforesaid schemes are low due to the involvement of large number of converter stages, and further in these schemes the component count is high and hence they face similar limitations as that of power electronic equalizer based scheme. Instead of ensuring MPP operation of each and every module, certain number of modules are connected in series to form a string and the so formed strings are then made to operate under MPP in [15], [16]. Even then there is not much reduction in overall component count and control complexity [6].

In order to simplify the control configuration and to reduce the component count, schemes reported in [17], [18] combine all the PV modules into two subarrays, and then each of the subarrays is made to operate at their respective MPP. However, the reported overall efficiency of both the schemes is poor. By introducing a buck and boost stage in SPGCT PV inverter, power extraction during MEC is improved in. Further, as a consequence of the presence of the intermediate boost stage, the requirement of series connected PV modules in a PV array has become less. In the schemes presented in [19]- [21], the switches of either the dc to dc converter stage or inverter stage operate at high frequency, as a result there is a considerable reduction in the size of the passive element count, thereby improving the operating efficiency of these schemes. Further, the reported efficiency of and is 1-2 % higher than that of.

An effort has been made in this paper to divide the PV modules into two serially connected subarrays and controlling each of the subarrays by means of a buck and boost based inverter so that optimum power evacuation from the subarrays is ascertained during MEC. This process of segregation of input PV array into two subarrays reduces the number of series connected modules in a subarray almost by half compared to that of the schemes proposed in.

The topological structure and control strategy of the proposed inverter ensure that the magnitude of leakage current associated with the PV arrays remains within the permissible limit. Further, the voltage stress across the active devices is reduced almost by half compared to that of the schemes presented in, hence very high frequency operation without increasing the switching loss is ensured. High frequency operation also leads to the reduction in the size of the passive elements. As a result the operating efficiency of the proposed scheme is high. The measured peak efficiency and the European efficiency (ηeuro) of the proposed scheme are found to be 97.65% and 97.02% respectively.

II. PROPOSED INVERTER AND ITS OPERATION

The schematic of the proposed Dual Buck & Boost based Inverter (DBBI) which is depicted in Fig. 1 is comprising of a dc to dc converter stage followed by an inverting stage. The dc to dc converter stage has two dc to dc converter segments, CONV1 and CONV2 to service the two subarrays, P V1 and P_{V2} of the solar PV array. The segment, CONV1 is consisting of the self-commutated switches, S_1 along with its anti-parallel body diode, D_1, S_3 along with its anti-parallel body diode, D3, the freewheeling diodes, D_{f1}, D_{f3} and the filter inductors and capacitors, L_1, C_{f1}, and C_{o1}.

Similarly, the segment, CONV2 is consisting of the self-commutated switches, S_2 along with its anti-parallel body diode, D_2, S_4 along with its anti-parallel body diode, D4, the freewheeling diodes, Df2, Df4 and the filter inductors and capacitors, L2, Cf2, and Co2. The inverting stage is consisting of the self-commutated switches, S5, S6, S7, S8, and their corresponding body diodes, D5, D6,D7 and D8 respectively. The inverter stage is interfaced with the grid through the filter inductor, Lg. The PV array to the ground parasitic capacitance is modeled by the two capacitors, Cpv1 and C pv2.

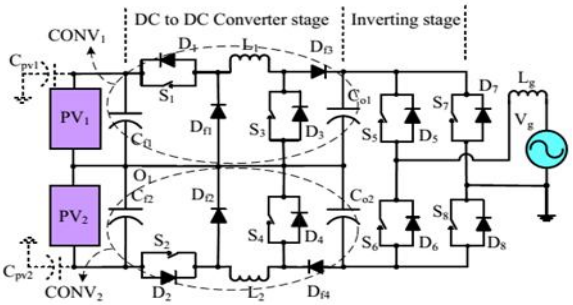

Fig. 1. Dual Buck & Boost based Inverter (DBBI)

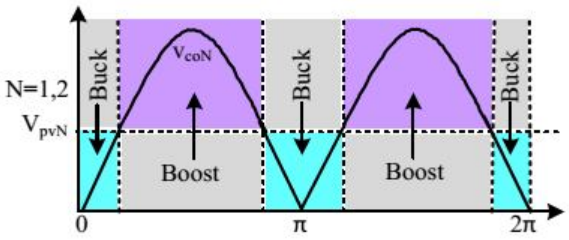

Fig. 2 Buck stage and Boost stage of the proposed inverter

Considering Fig. 2, CONV1 operates in buck mode when V pv1 ≥ vco1, while CONV2 operates in buck mode when V pv2 ≥ vco2. Vpv1, Vpv2 are the MPP voltages of P V1 and P V2 and v co1, vco2 are the output voltages of CONV1 and CONV2 respectively. During buck mode duty ratios of the switches, S1 and S2 are varied sinusoidally to ensure sinusoidal grid current (ig) while S3 and S4 are kept off. When Vpv1 < vco1, CONV1 operates in boost mode while CONV2 operates in boost mode when V pv2 < vco2. During boost mode duty ratios of the switches, S3 and S4 are varied sinusoidally to ensure sinusoidal i g while S1 and S2 are kept on throughout this mode. The sinusoidal switching pulses of the switches of CONV1 and CONV2 are synchronized with the grid voltage, v g to accomplish unity power factor operation. The switches, S5 and S8 are kept on and switches S6 and S7 are kept off permanently during the entire positive half cycle (PHC) while during entire negative half cycle (NHC), the switches, S_6 and S_7 are kept on and switches, S5 and S_8 are kept off permanently. All the operating states of the proposed inverter are depicted in Fig. 3.

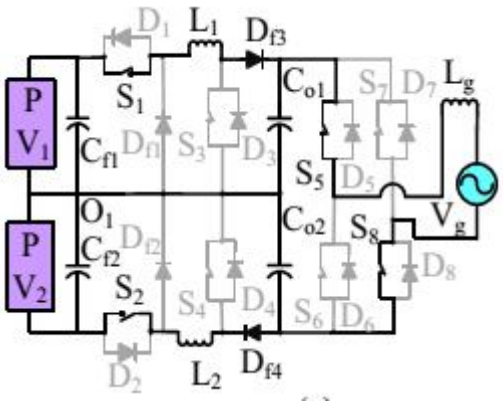

(a)

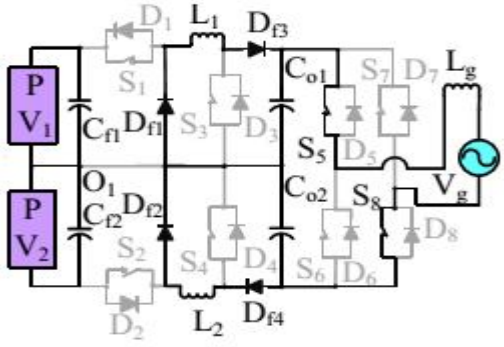

(b)

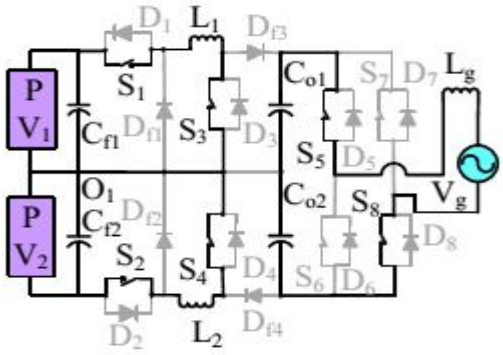

(c)

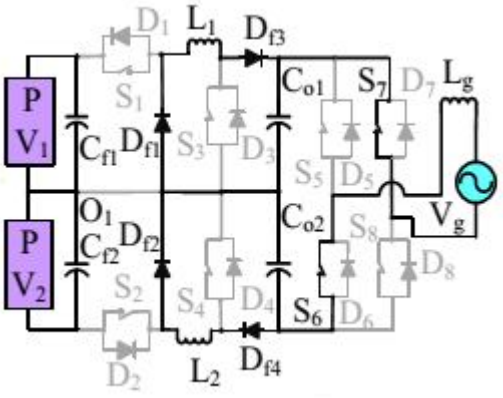

(d)

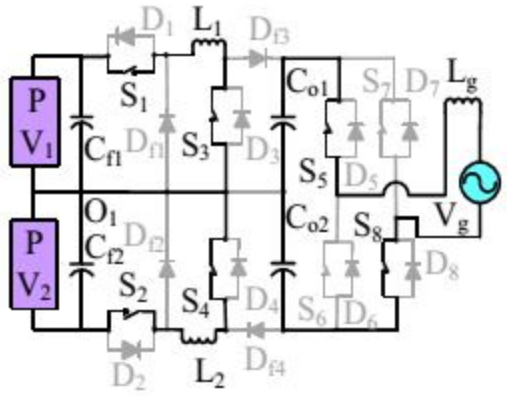

(e)

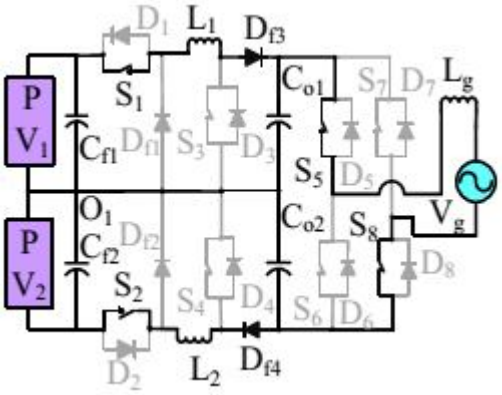

(f)

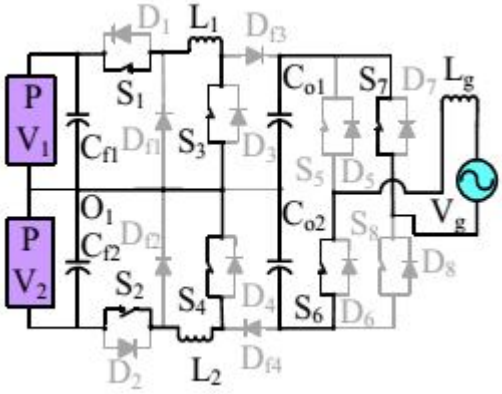

(g)

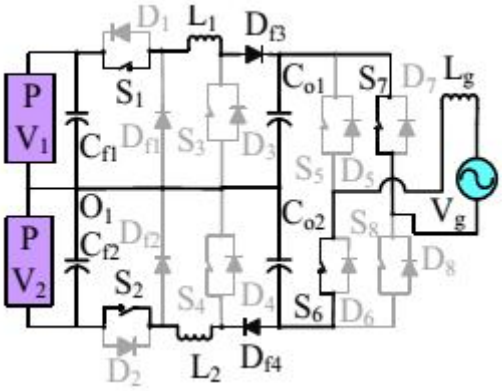

(h)

Fig. 3 Operating states of DBBI: (a) Active and (b) Freewheeling states in buck mode of PHC, (c) Active and (d) Freewheeling states in buck mode of NHC, (e) Active and (f) Freewheeling states in boost mode of PHC, (g) Active and (h) Freewheeling states in boost mode of NHC

When the insolation level and ambient temperature of sub array P V1 are different from that of P V2, the MPP parameter of the two subarrays, V_{pv1} and V_{pv2}, MPP current, I_{pv1} and I_{pv2} correspond to P_{V1} and P_{V2} respectively and power at MPP, P_{pv1} and P_{pv2} correspond to PV_1 and PV_2 respectively differ from each other. By considering that both the subarrays are operating at their respective MPP and neglecting the losses incurred in power processing stages, the average power involved with C o1 and Co2, Pco1 and Pco2 over a half cycle can be assumed equal to the power extracted from PV_1 and PV_2. Therefore,

$$P_{col} = P_{pv1} \,\&\, P_{co2} = P_{pv2} \qquad (1)$$

The power injected to the grid averaged over a half cycle, P_g can be written as

$$P_g = P_{pv1} + P_{pv2} \qquad (2)$$

Further, at any half cycle

$$v_g = v_{co1} + v_{co2} \qquad (3)$$

Hence, the instantaneous injected power to the grid, p_g can be written as

$$P_g = v_g i_g = (v_{co1} + v_{co2}) i_g \qquad (4)$$

Where in v_{co1} and v_{co2} denote the instantaneous quantities of V_{co1} and V_{co2} respectively. As ig is in-phase with vg,

$$i_g = \frac{P_g}{v_g} \qquad (5)$$

Where in V_g and I_g denote rms values of vg and i_g respectively. The power injected to the grid can be expressed as

$$P_g = \frac{1}{\pi}\int_0^{\pi} P_g d(wt)$$

$$P_g = \frac{1}{\pi}\int_0^{\pi} v_{co1} i_g d(wt) + \int_0^{\pi} v_{co2} i_g d(wt) \quad (6)$$

$$= P_{co1} + P_{co2} \quad (7)$$

As v co1 and vco2 are synchronized with vg. Hence

$$P_{co1} = \frac{1}{\pi}\int_0^{\pi} V_{co1m} \sin(wt)\ I_{gm}\ \sin(wt) d(wt)$$

$$= \frac{V_{co1m}\, I_{gm}}{2} \quad (8)$$

Similarly,

$$P_{co2} = \frac{V_{co2m}\, I_{gm}}{2} \quad (9)$$

Where in the amplitudes of v_{co1}, v_{co2} and i_g are denoted as V_{co1m}, V_{co2m} and I_{gm} respectively. Combining (1), (8) and (9) where in the amplitudes of vco1, vco2 and i_g are denoted as V co1m, V_{co2m} and I_{gm} respectively. Combining (1), (8) and (9)

$$V_{co1m} = \frac{2P_{pv1}}{I_{gm}} = \frac{\sqrt{2}P_{pv1}}{I_g} = \frac{\sqrt{2}P_{pv1}}{\left(P_g/V_g\right)} \quad (10)$$

$$V_{co2m} = \frac{2P_{pv2}}{I_{gm}} = \frac{\sqrt{2}P_{pv2}}{I_g} = \frac{\sqrt{2}P_{pv2}}{\left(P_g/V_g\right)} \quad (11)$$

Similarly by combining (2), (10) and (11),

$$V_{co1m} = \frac{V_m P_{pv1}}{P_{pv1}+P_{pv1}} \&\ V_{co2m} = \frac{V_m P_{pv2}}{P_{pv1}+P_{pv1}} \quad (12)$$

The voltage templates of vco1 and vco2 appear as full wave rectified sinusoidal waveform with amplitudes, V_{co1m} and V_{co2m} respectively. V_m is the amplitude of vg. It can be deduced from (12) that the magnitudes of V_{co1m} and Vco2m are decided by the power extracted from each of the subarray. If the power extracted from P_{V1} is less than P_{V2}, then V co1m < V_{co2m}, whereas Vco2m < Vco1m if power extracted from P_{V2} is less than PV1. During buck mode, the duty ratios, d1 of S1 and d2 of S2 vary sinusoidally with an amplitude d1m and d2m, wherein

$$d_{1m} = \frac{V_{co1m}}{V_{pv1}} \&\ d_{2m} = \frac{V_{co2m}}{V_{pv2}} \quad (13)$$

While during boost mode the duty ratios, d_3 of S3 and d_4 of S_4 vary sinusoidally with amplitude d3m and d4m, wherein

$$d_{3m} = 1 - \frac{V_{pv1}}{V_{co1m}} \&\ d_{4m} = 1 - \frac{V_{pv2}}{V_{co2m}} \quad (14)$$

The CONV1 and CONV2 are having the same output current i_g. Hence, the input side currents before getting filtered by input filter capacitors of CONV1, isw1 and CONV2, isw2 can be related with i_g in the buck mode by considering the switching cycle average of corresponding quantities as follows

$$\langle i_{sw1}\rangle_{T_s} = \langle d_1\rangle_{T_s}\langle i_g\rangle_{T_s} \quad (15)$$

$$\langle i_{sw2}\rangle_{T_s} = \langle d_2\rangle_{T_s}\langle i_g\rangle_{T_s} \quad (16)$$

Similarly by considering switching cycle average of corresponding quantities the relation between i_{sw1}, i_{sw2} and ig can be deduced during boost mode as

$$\langle i_{sw1}\rangle_{T_s} = \langle\frac{1}{1-d_3}\rangle_{T_s}\langle i_g\rangle_{T_s} \quad (17)$$

$$\langle i_{sw2}\rangle_{T_s} = \langle\frac{1}{1-d_4}\rangle_{T_s}\langle i_g\rangle_{T_s} \quad (18)$$

Therefore, it can be inferred from (12) and (13) that if the insolation level of P_{V1} is lower than that of P_{V2}, during buck mode, d1m < d2m, thereby hd1iT s < hd2iT s whereas during boost mode as per (12) and (14), d3m < d4m, thereby hd3iT s < hd4iT s . Hence, it can be concluded from (15), (16), (17) and (18) that in any operating mode, hisw1iT s < hisw2iT s , therefore $I_{pv1} < I_{pv2}$. Following the same argument, Ipv1 > I pv2 if the insolation level of PV1 is higher than that of P_{V2}. Considering Fig. 1 it can be noted that during operation in PHC, $v_{cpv1} = v_{co2} + V_{pv1}$, $v_{cpv2} = v_{co2} - V_{pv2}$ while during NHC vcpv1 = −vco1 + V_{pv1}, $v_{cpv2} = -v_{co1} - V_{pv2}$, wherein v_{cpv1} and v_{cpv2} are the voltages impressed across C_{pv1} and C_{pv2} respectively.

III. MATHEMATICAL MODEL OF THE PROPOSED SCHEME

A small signal modeling of the proposed inverter has been carried out for buck mode and boost mode of operation. Fig. 4(a) and (b) represent the equivalent circuit of the proposed inverter while it operates in buck mode whereas Fig. 4(c) and (d) represent the equivalent circuit of the converter while it operates in boost mode. R_{L1}, R_{L2}, R_g, R_{co1} and R_{co2} are the parasitic resistances of L_1, L_2, Lg, C_{o1} and C_{o2} respectively. As indirect grid current control method is adopted to control ig, the quantities i_{L1}, i_{L2}, v_{co1}, v_{co2} and i_g are considered to be the state variables. The state equations representing the buck mode of operation of the inverter are derived to be (19), (20) by considering the equivalent circuits of Fig. 4(a), (b) while the state equations for boost mode are derived

to be (21), (19) by considering the equivalent circuits of Fig. 4(c), (d).

$$\begin{bmatrix} \dot{i}_{L1}(t) \\ \dot{i}_{L2}(t) \\ \dot{v}_{co1}(t) \\ \dot{v}_{co2}(t) \\ \dot{i}_g(t) \end{bmatrix} = \begin{bmatrix} -\frac{R_{L1}+R_{co1}}{L_1} & 0 & -\frac{1}{L_1} & 0 & \frac{R_{co1}}{L_1} \\ 0 & -\frac{R_{L2}+R_{co2}}{L_2} & 0 & -\frac{1}{L_2} & \frac{R_{co2}}{L_2} \\ \frac{1}{C_{o1}} & 0 & 0 & 0 & -\frac{1}{C_{o1}} \\ 0 & \frac{1}{C_{o2}} & 0 & 0 & -\frac{1}{C_{o2}} \\ \frac{R_{co1}}{L_g} & \frac{R_{co2}}{L_g} & \frac{1}{L_g} & \frac{1}{L_g} & -\frac{R_{co1}+R_{co2}+R_g}{L_g} \end{bmatrix} \begin{bmatrix} i_{L1}(t) \\ i_{L2}(t) \\ v_{co1}(t) \\ v_{co2}(t) \\ i_g(t) \end{bmatrix} + \begin{bmatrix} \frac{1}{L_1} & 0 & 0 \\ 0 & \frac{1}{L_2} & 0 \\ 0 & 0 & 0 \\ 0 & 0 & 0 \\ 0 & 0 & -\frac{1}{L_g} \end{bmatrix} \begin{bmatrix} v_{pv1}(t) \\ v_{pv2}(t) \\ v_g(t) \end{bmatrix} \quad (19)$$

$$\begin{bmatrix} \dot{i}_{L1}(t) \\ \dot{i}_{L2}(t) \\ \dot{v}_{co1}(t) \\ \dot{v}_{co2}(t) \\ \dot{i}_g(t) \end{bmatrix} = \begin{bmatrix} -\frac{R_{L1}+R_{co1}}{L_1} & 0 & -\frac{1}{L_1} & 0 & \frac{R_{co1}}{L_1} \\ 0 & -\frac{R_{L2}+R_{co2}}{L_2} & 0 & -\frac{1}{L_2} & \frac{R_{co2}}{L_2} \\ \frac{1}{C_{o1}} & 0 & 0 & 0 & -\frac{1}{C_{o1}} \\ 0 & \frac{1}{C_{o2}} & 0 & 0 & -\frac{1}{C_{o2}} \\ \frac{R_{co1}}{L_g} & \frac{R_{co2}}{L_g} & \frac{1}{L_g} & \frac{1}{L_g} & -\frac{R_{co1}+R_{co2}+R_g}{L_g} \end{bmatrix} \begin{bmatrix} i_{L1}(t) \\ i_{L2}(t) \\ v_{co1}(t) \\ v_{co2}(t) \\ i_g(t) \end{bmatrix} + \begin{bmatrix} 0 & 0 & 0 \\ 0 & 0 & 0 \\ 0 & 0 & 0 \\ 0 & 0 & 0 \\ 0 & 0 & -\frac{1}{L_g} \end{bmatrix} \begin{bmatrix} v_{pv1}(t) \\ v_{pv2}(t) \\ v_g(t) \end{bmatrix} \quad (20)$$

$$\begin{bmatrix} \dot{i}_{L1}(t) \\ \dot{i}_{L2}(t) \\ \dot{v}_{co1}(t) \\ \dot{v}_{co2}(t) \\ \dot{i}_g(t) \end{bmatrix} = \begin{bmatrix} -\frac{R_{L1}}{L_1} & 0 & 0 & 0 & 0 \\ 0 & -\frac{R_{L2}}{L_2} & 0 & 0 & 0 \\ 0 & 0 & 0 & 0 & -\frac{1}{C_{o1}} \\ 0 & 0 & 0 & 0 & -\frac{1}{C_{o2}} \\ 0 & 0 & \frac{1}{L_g} & \frac{1}{L_g} & -\frac{R_{co1}+R_{co2}+R_g}{L_g} \end{bmatrix} \begin{bmatrix} i_{L1}(t) \\ i_{L2}(t) \\ v_{co1}(t) \\ v_{co2}(t) \\ i_g(t) \end{bmatrix} + \begin{bmatrix} \frac{1}{L_1} & 0 & 0 \\ 0 & \frac{1}{L_2} & 0 \\ 0 & 0 & 0 \\ 0 & 0 & 0 \\ 0 & 0 & -\frac{1}{L_g} \end{bmatrix} \begin{bmatrix} v_{pv1}(t) \\ v_{pv2}(t) \\ v_g(t) \end{bmatrix} \quad (21)$$

The state space averaging based technique is adopted as the grid frequency; f_g is adequately lower than the switching frequency, f_s. In order to simplify the analysis, V_{pv1}, V_{pv2} and vg are considered as stiff voltage sources, and the effect of input filter capacitors is neglected. The values of the system parameters are considered to be as follows: RL1 = R_{L2} = 0.12 Ω, R_g = 0.04 Ω, R_{co1} = R_{co2} = 0.26 Ω, V_{pv1} = V_{pv2} = 130 V. Considering symmetry in operation of CONV1 and CONV2, and by applying state space averaging technique to (19), (20) and (21), the simplified transfer functions of ig(s)/d(s), iL1(s)/d(s) and vco1(s)/d(s) in s-domain during buck mode are obtained as

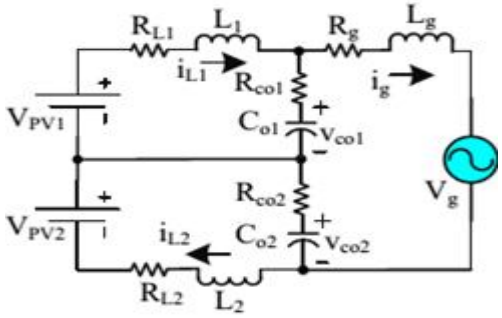

(a)

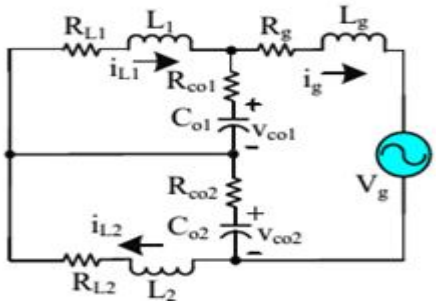

(b)

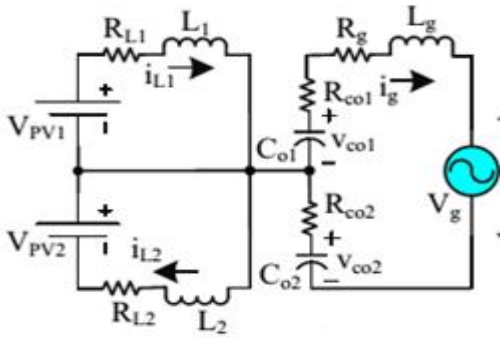

(c)

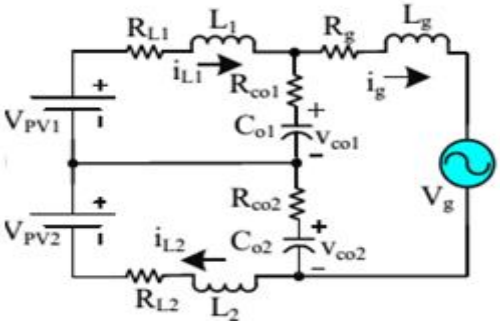

(d)

Fig. 4 Equivalent circuit in Buck mode (a) S1, S2 are ON (b) S1, S2 are OFF, in Boost mode (c) S3, S4 are ON (d) S_3, S_4 are OFF

IV. CONTROL STRATEGY OF THE PROPOSED SCHEME

The control strategy of the proposed scheme is depicted in Fig. 5. The controller is designed to fulfill the following objectives: i) both subarrays operate at their corresponding MPP simultaneously, ii) sensing of output voltages, vco1 and v co2 are not required, iii) ig is sinusoidal and is in-phase with v g throughout the operating range. Two separate MPP trackers and two proportional integral (PI) controllers are employed to determine the value of P pv1 and P_{pv2} which are required

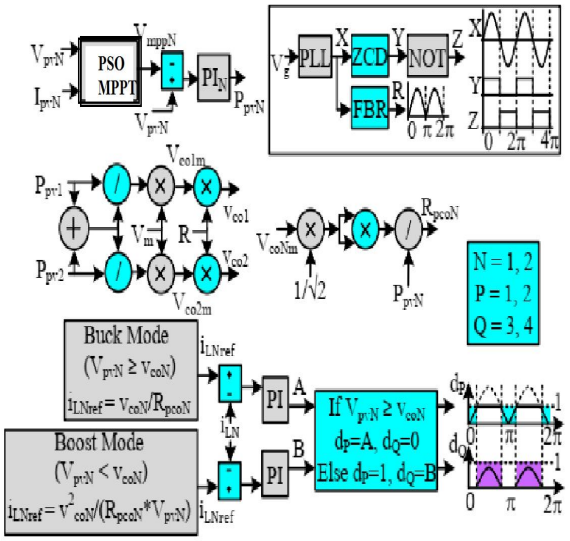

Fig. 5 Control configuration of the proposed inverter to estimate V_{co1m} and V_{co2m}

Using (12), V_{co1m} and V_{co2m} are determined where the information of V m is obtained from the phase locked loop (PLL). A rectified version of a unity sinusoidal function, R is generated from a unity sinusoidal function, X, synchronized with vg, and is obtained from the same PLL. R is multiplied with Vco1m and Vco2m to estimate v co1 and vco2. Hence, two voltage sensors which otherwise would have been required to determine vco1 and vco2 get eliminated. V_{pv1} and v_{co1} are compared to decide about the mode of operation (buck mode or boost mode) of CONV1, while V_{pv2} and v_{co2} are compared to determine the mode of operation of CONV2. RMS values of vco1 and vco2 are estimated which are then subsequently squared and are then divided by P_{pv1} and P_{pv2} to obtain the emulated effective resistances, R_{pco1} and R_{pco2} of the two component converters. Subsequently the reference current, i_{L1}ref of L_1 and the reference current, i_{L2}ref of L_2, are synthesized by utilizing (22) in the buck mode,

$$i_{L1ref} = \frac{v_{co1}}{R_{pco1}} \& i_{L2ref} = \frac{v_{co2}}{R_{pco2}} \quad (22)$$

While for boost mode (23) is used to generate iL1ref and i_{L2ref}.

$$i_{L1ref} = \frac{{v_{co1}}^2}{R_{pco1}V_{pv1}} \& i_{L1ref} = \frac{{v_{co2}}^2}{R_{pco2}V_{pv2}} \quad (23)$$

The sensed inductor currents, i_{L1} and i_{L2} are compared with their corresponding references iL1ref and i_{L2ref}. The errors so obtained are processed through two separate PI controllers to generate the required sinusoidal duty ratios for the switches, S1 and S2 during buck mode. Similarly, two separate PI controllers are engaged to process the generated errors to synthesize required sinusoidal duty ratios for switches S3 and S4 during boost mode.

V. SELECTION OF L1, L2, L_g & Co1, Co2

In order to select the value of the filter elements, L_1, L_2, L_g & C_{o1}, C_{o2} the design principle given in is followed and the buck mode of operation for the inverter is considered. Values of L_1 and L_2 are obtained from the expression given in

$$L_1 = \frac{V_{pv1}}{4\Delta I_{L1} f_s} \& L_2 = \frac{V_{pv2}}{4\Delta I_{L2} f_s} \quad (24)$$

wherein, V_{pv1} = V_{pv2} = 200 V, percentage peak to peak ripple of i_{L1} and i_{L2}, ΔI_{L1} and ΔI_{L2} are considered as 15% of rated peak current.

The values of C_{o1} and C_{o2} are obtained from the expression given in.

$$C_{o1} = \frac{xP_{co1}}{2\pi f_g {V_{co2}}^2} \& C_{o1} = \frac{xP_{co2}}{2\pi f_g {V_{co2}}^2} \quad (25)$$

VI OVERVIEW OF THE PSO ALGORITHM

PSO is a swarm intelligence optimization algorithm developed by Eberhart and Kennedy in 1995. In this algorithm, several cooperative agents are used, and each agent exchanges information obtained in its respective search process. Each agent, referred to as a particle, follows two very simple rules, i.e., to follow the best performing particle, and to move towards the best conditions found by the particle itself. By this way, each particle ultimately evolves to an optimal or close to optimal solution. The standard PSO m

$$v_i\,(k+1) = wv_i(k) + c_1 r_1 . (P_{best.i} - x_i(k)) + c_2 r_2 . (g_{best.i} - x_i(k)) \quad (26)$$

$$v_i\,(k+1) = x_i(k) + v_i\,(k+1) \quad (27)$$

I=1,2,……,N

Where x_i is the position of particle i; vi is the velocity of particle i; k denotes the iteration number; w is the inertia weight; r_1 and r_2 are random variables uniformly distributed within [0,1]; and c_1, c_2 are the cognitive and social coefficient, respectively. The variable p_{best},i is used to store the best position that the i-th particle has found so far, and g_{best} is used to store the best position of all the particles.

Step1.

PSO initialization Particles are usually initialized randomly following a uniform distribution over the search space, or are initialized on grid nodes that

cover the search space with equidistant points. Initial velocities are taken randomly.

Step2. Fitness Evaluation Evaluate the fitness value of each particle. Fitness evaluation is conducted by supplying the candidate solution to the objective function.

Step3. Update individual and global best data Individual and global best fitness values (pbest,i and gbest) and positions are updated by comparing the newly calculated fitness values against the previous ones, and replacing the pbest,i and gbest as well as their corresponding positions as necessary.

Step4. Update velocity and position of each particle the velocity and position of each particle in the swarm is updated using Eq. (2) and (3).

Step5. Convergence Determination Check the convergence criterion. If the convergence criterion is met, the process can be terminated; otherwise, the iteration number will increase by 1 and goto step 2.

VII. SIMULATION STUDY

To demonstrate the efficacy of the proposed inverter a PV array consisting of two PV subarrays while each of the subarray having four series connected Canadian solar polycrystalline modules 'CS6P-165PE' is considered. The MPP parameters of each subarray at standard test condition (STC) are as follows: $V_{pv1} = V_{pv2} = 116$ V, $I_{pv1} = I_{pv2} = 5.7$ A and P $p_{v1} = P_{pv2} = 661$ W. The parameters which are used to simulate the proposed inverter are indicated in Table I.

TABLE I
Employed Parameters/Elements For Simulation And Experimental Purpose

V_g and f_g	220 V and 50 Hz
L_1, L_2, L_g & C_{o1}, C_{o2}	0.6 mH, 0.6 mH, 0.4 mH & 5 μF, 5 μF
C_{pv1} and C_{pv2}	0.1 μF
MPPT Algorithm	Incremental Conductance
Mosfets (S_1-S_8)	IPW60R041C6
Diodes (D_{f1}-D_{f4})	MBR40250
f_s of S_1-S_4 & f_s of S_5-S_8	50 kHz & 50 Hz
Digital Signal Controller	TMS320F28335

Matlab Simulink platform is utilized to simulate the performance of the proposed inverter.The variation in insolation level and temperature with respect to time which is considered for the two subarrays to demonstrate the effectiveness of the proposed inverter are tabulated in Table II.

TABLE II
Estimated Variations of Different Quantities during Applied Variations on Insolation and Temperature of Two Subarrays

Time in Second	0-1	1-2	2-3	3-4	4-5	5-6	6-7	7-8
Insol. in PV_1 (kW/m^2)	0.5	0.6	0.7	0.8	0.9	1.0	1.0	1.0
Insol. in PV_2 (kW/m^2)	0.8	0.8	0.8	0.8	0.8	0.8	0.8	0.8
Temp. in PV_1 (°C)	25	25	25	25	25	25	30	35
Temp. in PV_2 (°C)	25	25	25	25	25	25	25	25
P_{pv1} (W)	331	397	463	529	595	661	638	621
P_{pv2} (W)	529	529	529	529	529	529	529	529
I_{gm} (A)	5.5	6.0	6.4	6.8	7.2	7.7	7.5	7.4
V_{co1m} (V)	120	133	147	155	165	173	170	168
V_{co2m} (V)	191	178	164	156	146	138	141	143
I_{L1m} (A)	5.7	7	8.1	9	10.3	11.4	11	10.7
I_{L2m} (A)	9	9	9	9	9	9	9	9

Estimated variation of P_{pv1}, P_{pv2} along with the other parameters I_{gm}, V_{co1m}, V_{co2m}, peak of i_{L1} (I_{L1m}) and peak of i_{L2} (I_{L2m}) are also indicated in the same table. Fig. 6(a)-(c) represents the variation of P_{pv1}, P_{pv2}, V_{pv1}, V_{pv2}, I_{pv1}, I_{pv2} of the two subarrays and also demonstrates the ability of the proposed inverter to operate the two subarrays simultaneously at their respective MPP. Variation in ig, i_{L1}, i_{L2}, vco1 and v_{co2} along with their magnified versions for two different insolation levels are depicted in Figs. 7 to 9. The estimated values of the aforementioned quantities as tabulated in Table II conform to that of obtained through simulation studies thereby ensuring the viability of the proposed scheme.

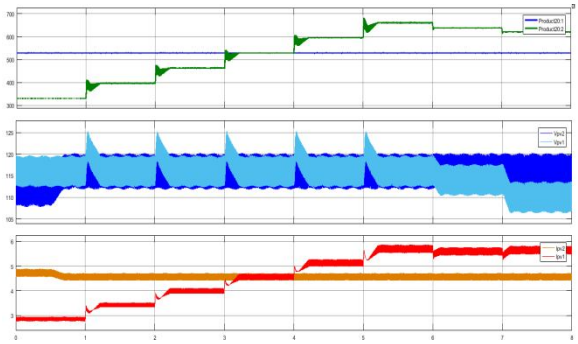

Fig. 6. Simulated waveform: Variation in (a) p_{pv1} and p_{pv2}, (b) v_{pv1} and v_{pv2}, (c) i_{pv1} and i_{pv2} during entire range of operation

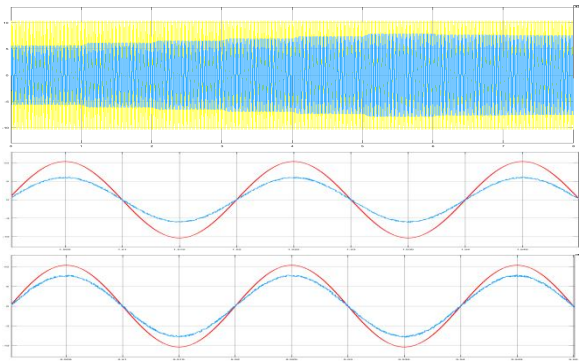

Fig. 7.Simulated waveform: v_g and i_g and their magnified views

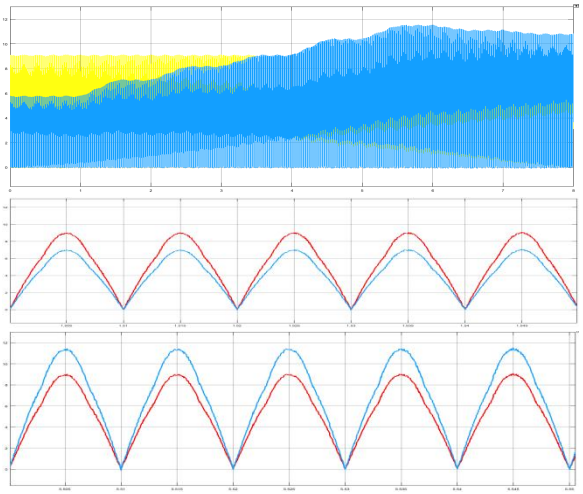

Fig. 8.Simulated waveform: i_{L1} and i_{L2} and their magnified views

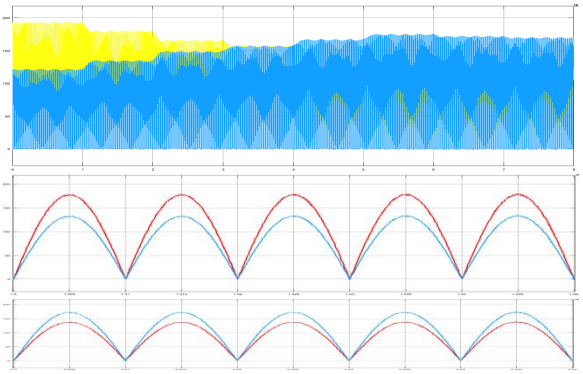

Fig. 9 Simulated waveform: vco1 and vco2 and their magnified views

VII. CONCLUSION

A solitary phase grid associated transformerless buck and boost based PV inverter which can work two subarrays at their particular PSO MPPT based proposed in this paper. PSO procedures can produce fantastic arrangements inside shorter figuring time and stable union qualities than other stochastic methods.The attractive highlights of this inverter were I) impact of confounded natural conditions on the PV array could be managed in a compelling way, ii) working proficiency accomplished, ηeuro = 97.02% was high, iii) decoupled control of component converters was conceivable, iv) basic MPPT calculation was utilized to guarantee MPP operation for the component converters, v) leakage current related with the PV arrays was inside the farthest point referenced in VDE 0126-1-1. Mathematical examination of the proposed inverter prompting the advancement of its little signal model was completed. The model to choose the estimations of the output filter components was displayed. The plan was approved via completing definite simulation contemplates.

REFERENCES

[1] T. Shimizu, O. Hashimoto, and G. Kimura, “A novel high-performance utility-interactive photovoltaic inverter system,” IEEE Trans. Power Electron., vol. 18, no. 2, pp. 704-711, Mar. 2003.

[2] S. V. Araujo, P. Zacharias, and R. Mallwitz, “Highly efficient single phase transformerless inverters for grid-connected photovoltaic systems,” IEEE Trans. Ind. Electron., vol. 57, no. 9, pp. 3118-3128, Sep. 2010.

[3] B. Ji, J. Wang, and J. Zhao, “High-efficiency single-phase transformerless PV H6 inverter with hybrid modulation method,” IEEE Trans. Ind. Electron., vol. 60, no. 5, pp. 2104-2115, May 2013.

[4] R. Gonzalez, E. Gubia, J. Lopez, and L. Marroyo, “Transformerless single phase multilevel-based photovoltaic inverter,” IEEE Trans. Ind. Electron., vol. 55, no. 7, pp. 2694-2702, Jul. 2008.

[5] H. Xiao and S. Xie, “Transformerless split-inductor neutral point clamped three-level PV grid-connected inverter,” IEEE Trans. Power Electron., vol. 27, no. 4, pp. 1799-1808, Apr. 2012.

[6] A. Bidram, A. Davoudi, and R. S. Balog, “Control and circuit techniques to mitigate partial shading effects in photo voltaic arrays,” IEEE J. Photovolt., vol. 2, no. 4, pp. 532-546, Oct. 2012.

[7] N. D. Kaushika, and N. K. Gautam, “Energy yield simulations of interconnected solar PV arrays,” IEEE Trans. Energy Convers., vol. 18, no. 1, pp. 127-134, Mar. 2003.

[8] H. Patel, and V. Agarwal, “Maximum power point tracking scheme for PV systems operating under partially shaded conditions,” IEEE Trans. Ind. Electron., vol. 55, no. 4, pp. 1689-1698, Apr. 2008.

[9] D. Nguyen, and B. Lehman, "An adaptive solar photovoltaic array using model-based reconfiguration algorithm," IEEE Trans. Ind. Electron., vol. 55, no. 7, pp. 2644-2654, Jul. 2008.
[10] G. V.-Quesada, F. G.-Gispert, R. P.-Lopez, M. R.-Lumbreras, and A. C.- Roca, "Electrical PV array reconfiguration strategy for energy extraction improvement in grid-connected PV systems," IEEE Trans. Ind. Electron., vol. 56, no. 11, pp. 4319-4331, Nov. 2009.
[11] L. F. L. Villa, T.-P. Ho, J.-C. Crebier, and B. Raison, "A power electronics equalizer application for partially shaded photovoltaic modules," IEEE Trans. Ind. Electron., vol. 60, no. 3, pp. 1179-1190, Mar. 2013.
[12] P. Sharma, and V. Agarwal, "Maximum power extraction from a partially shaded PV array using shunt-series compensation," IEEE J. Photovolt., vol. 4, no. 4, pp. 1128-1137, Jul. 2014.
[13] N. Femia, G. Lisi, G. Petrone, G. Spagnuolo, and M. Vitelli, "Distributed maximum power point tracking of photovoltaic arrays: novel approach and system analysis," IEEE Trans. Ind. Electron., vol. 55, no. 7, pp. 2610-2621, Jul. 2008.
[14] C. Olalla, C. Deline, D. Clement, Y. Levron, M. Rodriguez, and D. Maksimovic, "Performance of power-limited differential power processing architectures in mismatched PV systems," IEEE Trans. Power Electron., vol. 30, no. 2, pp. 618-630, Feb. 2015.
[15] E. Karatepe, T. Hiyama, M. Boztepe, and M. C. olak, "Voltage based power compensation system for photo voltaic generation system under partially shaded insolation conditions," Energy Convers. and Manage., vol. 49, pp. 2307-2316, Aug. 2008.

Student Details :

Name: **KAYA SRINIVASARAO**

Mr.KAYA SRINIVASARAO was born in Srikakulam ,AP on Septembers 10, 1992 . He graduated from the Jawaharlal Nehru Technological University Hyderabad ,India in 2014 . His special fields of interest included PLC . Presently He is studying M.Tech in Power Electronics & Drives at MVR College of Engineering and Technology Paritala , Vijayawada, AP, India

Faculty Details:

Name: Kiran Kumar Konda

Mr. : Kiran Kumar Konda was born Guntur,AP, on May 06 1988. He received B-Tech degree in NCET Engineering college Krishna india in 2009 . He received M-Tech in Power Electronics & Drives at LBRC Engineering college , Mylavaram , Krishna India in 2014 . Presently He is working as a Asst Prof in MVR College of Engineering, Paritala . So far he is having 5 Years of Teaching Experience . His special fields of interest included Power Electronics.